

# Development of Effective Procedures for Stormwater Thermal Pollution Potential Risk Mapping

Clinton J. Martin

Thesis submitted to the faculty of the Virginia Polytechnic Institute and State University in  
partial fulfillment of the requirements for the degree of

Master of Science  
In  
Civil Engineering

Randel L. Dymond, Chair  
Clayton C. Hodges  
Kevin D. Young

December 15<sup>th</sup>, 2016  
Blacksburg, VA

Keywords: Stormwater management, Temperature, Thermal pollution, Geographic information systems, Risk mapping

# Development of Effective Procedures for Stormwater Thermal Pollution Potential Risk Mapping

Clinton J. Martin

## ACADEMIC ABSTRACT

Thermal pollution of waterbodies from stormwater runoff in urban catchments is a growing concern among municipalities in the United States. The U.S. Environmental Protection Agency (EPA) maintains regulatory criteria for temperature of waters of the U.S. as aquatic life depends on an ecosystem that maintains a healthy temperature regime. To seek effective means for mitigation of thermal pollution, a municipality must first identify the sources of thermal pollution in its waterbodies. This study predicts areas within an urban catchment in the Town of Blacksburg, VA that may be sources of thermal pollution in stormwater runoff by investigating indicators of thermal pollution potential (TPP) through spatial analyses of land cover types and runoff travel times in a geographic information system (GIS) environment. Results of the study provide a TPP risk map that identifies hotspots near areas of high imperviousness within small subwatersheds in the study area along with recommendations for authorities interested in pursuing TPP risk mapping as a tool to guide thermal pollution mitigation efforts or land use planning.

# Development of Effective Procedures for Stormwater Thermal Pollution Potential Risk Mapping

Clinton J. Martin

## PUBLIC ABSTRACT

Thermal pollution of waterbodies occurring from heated stormwater runoff in urban catchments is a growing concern among municipalities in the United States. The U.S. Environmental Protection Agency (EPA) maintains regulatory criteria for temperature of waters of the U.S. as many species of aquatic life depend on an environment that maintains water temperatures below a certain threshold. Thermal pollution from urban stormwater runoff threatens the livelihoods of cold-water fish species, like trout, among other species of wildlife. In order to reduce thermal pollution loading to its streams, a municipality or regulatory authority must first identify the sources of thermal pollution in its waterbodies. This study predicts areas within an urban watershed in the Town of Blacksburg, VA that may be sources of thermal pollution in stormwater runoff by investigating indicators of thermal pollution potential (TPP) through an analysis of land cover types and runoff flow patterns in a geographic information system (GIS) environment. Results of the study provide a theoretical foundation for TPP risk mapping with recommendations for authorities interested in pursuing TPP risk mapping as a tool to guide and focus efforts toward reduction of thermal pollution and land planning.

## ACKNOWLEDGEMENTS

The efforts of many individuals were invaluable to this thesis project, particularly the guidance and support of my committee. I consider myself very fortunate to have had a committee so dedicated and involved that each member played a role in mentoring me in multiple aspects of life, not only research. I want to thank Randy Dymond for serving as my committee chair and for his exemplary leadership that I hope to one day emulate. I want to thank Clay Hodges for going above and beyond the expectations of a committee member by showing a genuine interest in my research, asking questions throughout, and working with me directly to iron out the kinks along the way. I also want to thank Kevin Young for his patience and understanding in his dual-role as committee member and supervisor while I balanced thesis work with teaching.

Outside my committee, I would like to extend sincerest gratitude to two other mentors, Marcus Aguilar and Walter McDonald who provided both encouragement and inspiration. Also deserving of my gratitude are the rest of the members of my research group, both old and new, and especially Lauren Cetin for her additional support when I needed to focus on my thesis. Last but not least, I would like to thank my family, friends, and the Hokie Nation for their love and encouragement; I surely would not have been able to succeed without them.

# TABLE OF CONTENTS

List of Figures .....	vi
List of Tables .....	vii
I. Introduction .....	1
A. Background .....	1
B. Problem Statement .....	3
C. Purpose and Objectives .....	4
II. Literature Review .....	5
A. Effects of Urbanization on Stream Temperature.....	5
B. Stormwater Thermal Pollution Indicators .....	6
1. Simulating Stormwater Runoff Volume and Temperature .....	6
2. Land Cover Temperature .....	7
C. Summary .....	8
III. Development of Effective Procedures for Stormwater Thermal Pollution Potential Risk Mapping .....	8
A. Introduction .....	8
B. Background .....	9
C. Research Purpose .....	10
D. Methods.....	11
1. Data Sources.....	12
2. Thermal Pollution Potential Development.....	13
3. Thermal Pollution Potential Risk Map Development .....	20
E. Results and Discussion .....	24
1. K-Value Sensitivity Analysis.....	29
F. Conclusions.....	30
IV. Conclusion .....	31
A. Implications .....	31
B. Future Work .....	32
C. Final Words .....	34
References.....	35
Appendix A – Method 2 Python Scripts.....	38

## LIST OF FIGURES

Figure 3-1. Stormwater runoff thermal energy heat budget ignoring weather-related inputs on a) a single land cover cell (adapted from Kieser 2004) and b) a theoretical watershed of nine land cover grid cells .....	14
Figure 3-2. Watershed boundaries developed from a) Method 1, b) Method 2, and c) Method 3. ....	26
Figure 3-3. Risk maps of a) $TPP_{LC}$ derived from DLCDC (2013), b) TPP from Method 2, and c) TPP from Method 3. All are at 1-m spatial resolution.....	27
Figure 3-4. Comparison of TPP frequency distribution across the entire Central Stroubles watershed for a) Method 2 at 10-m resolution, b) Method 2 at 1-m resolution, c) Method 3 at 10-m resolution, and d) Method 3 at 1-m resolution. ....	28
Figure 3-5. Comparison of TPP frequency distribution using Method 2 at 1-m spatial resolution, for a) Subwatershed 1 and b) Subwatershed 2.....	29
Figure 3-6. Comparison of TPP frequency distribution from Method 2 at 1-m spatial resolution using separate cooling constant K values, where a) $K=0.03$ and b) $K=0.04$ . ....	30

## LIST OF TABLES

Table 3-1. TPP <sub>LC</sub> categories for DLCD (2013) and NLCD (2011) land cover types assigned using temperature data from Herb et al. (2008).....	16
Table 3-2. Manning's n and channel k values assigned to DLCD (2013) land cover types.....	21

# I. INTRODUCTION

## A. BACKGROUND

Thermal pollution of water bodies in urban catchments is a growing water quality concern in the United States. The U.S. Environmental Protection Agency (EPA) and state agencies such as the Virginia Department of Environmental Quality (DEQ) maintain regulatory criteria for various water quality parameters including temperature (USEPA 2016; VADEQ 2014; Virginia Administrative Code 1998). According to the Virginia DEQ Final 2014 305(b)/303(d) Water Quality Assessment Integrated Report (VADEQ 2014), there are many bodies of water identified as impaired for aquatic life due to temperatures in excess of these criteria. Twenty-nine percent of all assessed rivers/streams (6,479 miles), 43% of assessed lake acres (48,555 acres), and 86% of assessed estuarine waters (2,114 square miles) are impaired for aquatic life using dissolved oxygen, pH, temperature, chlorophyll a, nutrients, water column and sediment toxics, toxicity tests, benthics, and submerged aquatic vegetation as indicators for the aquatic life use (VADEQ 2014). In the New River Basin, 13% of river impairments are due to temperature, which is higher than impairments due to benthics, PCBs in fish tissue, mercury in fish tissue, and sedimentation. Temperature is second only to bacteria causes, which are represented in 85% of river impairments (VADEQ 2014, Table 4.3-17).

Aquatic life is dependent on ecosystems that maintain a healthy temperature regime. Temperature assumes a controlling, or at least a modifying role, in most aspects of insect development (i.e. macroinvertebrates) (Vannote and Sweeney 1980). Additionally, water temperature is one of the most important environmental stressors affecting fish. Temperature regimes influence migration, egg maturation, spawning, incubation success, growth, inter- and intraspecific competitive ability, and resistance to parasites, diseases, and pollutants (Armour 1991). Salmonid species, like trout, are among the fish most sensitive to water temperature fluctuations (Jones et al. 2007). Brown Trout (*Salmo trutta*), for example, have an optimum temperature range of 7 to 17 °C and become stressed at temperatures above 19 °C, while temperatures above 26 °C are considered lethal (Roa-Espinosa et al. 2003). While most fish species can tolerate seasonal changes in temperature, rapid spikes in temperature are particularly lethal (Jones et al. 2007).



Due to these negative effects on stream ecology, municipalities are seeking effective means to predict the sources of thermal pollution within their jurisdictional boundaries so that they may efficiently allocate resources for mitigation techniques such as installation of best management practices (BMPs) that have been shown to reduce thermal loading of stormwater runoff (Jones et al. 2007; Long and Dymond 2013). To more effectively implement minimization and mitigation strategies, the salient factors for predicting sources of thermal pollution in surface runoff must be determined prior to application of models evaluating areas of high thermal load potential within urban areas.

Previous studies have shown that urbanization has a strong thermal impact on streams (Roa-Espinosa et al. 2003; Pluhowski 1970). Urbanization affects many elements of importance to stream heat budgets, such as removal of riparian vegetation that would otherwise provide shading and evapotranspiration, decreased groundwater contribution, and increased stormwater runoff that has been heated by contact with warm surfaces (e.g. the “heat island” effect associated with urbanization) (Roa-Espinosa et al. 2003; Pluhowski 1970; Paul and Meyer 2001; Kieser 2004; Kim 1992). According to the study performed by Pluhowski (1970), summertime storms resulted in increased temperature pulses of urban streams by up to 10-15 °C when compared with forested streams in Long Island, New York. Pluhowski also asserted that the precise effect that stormwater runoff will have on the temperature of downstream reaches is a function of the relative volume of stormwater runoff to streamflow, the ambient temperature differences between the two, and whether the stormwater runoff enters the stream as a concentrated mass or whether it is distributed along the channel. Urbanization increases stormwater runoff volume and decreases riparian vegetation – which also affects flow regime, increasing the likelihood of concentrated stormwater entering the stream (Pluhowski 1970; Jones et al. 2007). The effects of the temperature differences and relative volume of stormwater runoff seem to play the largest roles (Jones et al. 2007; Wardynski et al. 2013).

Several studies have been successfully performed to estimate stormwater runoff temperature in urban catchments to determine its effect on stream temperature (Herb et al. 2006; Herb et al. 2007; Janke et al. 2008; Herb et al. 2008). The studies all concluded that land surface temperature plays a significant role in the stormwater runoff temperatures entering the stream.

Models that estimate land surface temperature are useful in determining stormwater runoff temperature, since the two parameters are directly related. According to Herb et al. (2008), land surface temperature varies by land cover type. Therefore, the land cover types present in an urban catchment can be used to determine the extent to which thermal pollution may potentially occur in a receiving stream from a particular point of interest.

## B. PROBLEM STATEMENT

The current literature provides studies that predict stormwater runoff rates and temperatures to quantify thermal load impacts by taking into account radiative, convective, evaporative, and conductive heat fluxes at the surface (Janke et al. 2008; Roa-Espinosa et al. 2003). These models require a significant number of input parameters including, but not limited to, rainfall temperature and volume, initial surface temperature, and various other surface properties such as thermal diffusivity, heat capacity, area, slope, and roughness (Janke et al. 2008). Each of these models require different inputs for different rainfall events and multiple iterations for varying surfaces. While these models are effective predictors of stormwater runoff thermal load for a specific rainfall event and surface properties, there remains a need for a simpler procedure – independent of specific rainfall events – to estimate potential locations where thermal pollution might occur throughout a watershed. No literature was found that defines methods for quantifying this potential for thermal pollution along surfaces in an urban watershed. This study develops several procedures that estimate thermal pollution potential (TPP) – a numerical score assigned to areas of interest based on the relative potential for contribution of thermal pollution to the nearest receiving inlet or watershed outlet (pour point) based on hydrothermal processes and independent of weather conditions. The resultant TPP values are spatially analyzed in a GIS to produce a TPP risk map. This study also determines the impact of using varying types of input data to determine the transferability of these procedures to other municipalities outside of the study area. The ultimate goal of this research is to provide fairly simple procedures to create a TPP risk map for identifying areas with high potential for causing thermal pollution.

## C. PURPOSE AND OBJECTIVES

Once areas within watersheds that are prone to thermally polluting receiving waters are identified, potential locations for stormwater BMPs that are able to partially mitigate the effects of thermal pollution can be identified through use of the TPP risk map. BMPs such as bioretention cells have been shown to reduce runoff temperature by passing water through cooler subsurface media (Wardynski et al. 2013; Long and Dymond 2013). Additional types of BMPs have been shown to mitigate thermal pollution by runoff volume reduction (e.g. pervious pavers) (Jones et al. 2007; Wardynski et al. 2013). The TPP risk map could be used as an action plan element for reduction of thermal pollution to a municipality's receiving streams.

The purpose of this study is to develop effective procedures for thermal pollution potential (TPP) risk mapping that can be used by a municipality to create a TPP risk map. To that end, the proposed research objectives for this thesis research are to:

1. Determine factors influencing thermal pollution and how these factors have been used for thermal pollution estimation through review of current literature
2. Evaluate factors influencing stormwater thermal pollution for their effectiveness and logical application to TPP and TPP risk mapping based on relative performance and data availability
3. Develop TPP and TPP risk maps for a single case study through spatial analyses of applicable factors
4. Analyze results for sensitivity to different methodologies and data sources
5. Recommend effective procedures for TPP risk mapping

## II. LITERATURE REVIEW

### A. EFFECTS OF URBANIZATION ON STREAM TEMPERATURE

Urbanization intensifies land for human use by way of development. Roads, buildings, and sidewalks are dominant land cover types in urbanized areas. These land cover types have a distinctly different set of hydrologic and thermal properties as compared to typical pre-development land cover types such as forest, shrubs, and wetlands. These modifications to the natural environment, therefore, have significant impacts on waters within the urban landscape. The extensive and ever-increasing urbanization trends in the U.S. and the world further compound these impacts. Over 130,000 km of streams and rivers in the U.S. are impaired by urbanization (Paul and Meyer 2001), which makes urbanization a major cause of stream impairment, second only to agriculture despite urban areas' significantly smaller land cover footprint. In their review of multiple previous studies, Paul and Meyer (2001) synthesize the effects of urbanization on stream ecology into two categories: 1) physical responses to hydrology, geomorphology, and temperature and 2) biological responses to fish and invertebrates.

While the effects of urbanization on stream ecology extend beyond the realm of thermal pollution, many of these effects coincide with each other and combine to result in greater thermal pollution pulses and variations of stream temperature than in natural conditions. Specifically, the physical responses to hydrology and geomorphology both influence urbanization's effect on stream temperature. The responses to hydrology include increased stormwater runoff volume, increased temperature of stormwater runoff, decreased time of concentration, and decreased groundwater infiltration (Paul and Meyer 2001; Pluhowski 1970; Roa-Espinosa et al. 2003). The responses to geomorphology include removal of riparian vegetation and channel incising/bank instability (Paul and Meyer 2001; Pluhowski 1970). Stormwater runoff volume and temperature together determine the thermal energy of the stormflow portion of streamflow; an increase of both dramatically increases the thermal energy received by the stream. Decreased time of concentration shortens the time to peak on a storm hydrograph, thereby increasing stormflow influence on a stream's short-term temperature regime. Decreased groundwater infiltration results in decreased groundwater recharge, thus reducing groundwater contribution to streams

(Pluhowski 1970), causing a long-term decrease in the baseflow portion of streamflow. Removal of riparian vegetation causes a reduction in evapotranspiration and shading on and nearby the stream, exposing the stream to direct solar radiation (Swift and Messer 1971). Channel incising/bank instability increases the likelihood of concentrated stormwater entering the stream as opposed to sheet flow distributed along the channel.

The above responses to hydrology and geomorphology of urban streams tend to increase the influence of stormwater runoff on the temperature regime, resulting in greater seasonal and diurnal temperature fluctuations. Urban streams experience higher average temperatures in the summer and lower average temperatures in the winter. Greater diurnal temperature fluctuation is most prevalent in the summer when solar radiation is high and summer storms give way to thermally polluted surface runoff.

## **B. STORMWATER THERMAL POLLUTION INDICATORS**

Since urban streams are heavily dependent on stormflow, stormwater thermal pollution plays a significant role on the temperature regime. As defined earlier, stormwater thermal pollution is the total thermal energy held by the stormwater runoff that enters the stream. Stormwater runoff volume and temperature determine the thermal energy load delivered; if these values can be determined, so can the magnitude of thermal pollution. Several studies developed models to estimate stormwater runoff volume and temperature in various conditions for the purpose of estimating stormwater thermal pollution (Haq and James 2002; Janke et al. 2009; Kieser et al. 2004; Roa-Espinosa et al. 2003). These models and others are also referenced in Janke et al (2009) and Sabouri et al (2013). While there are differences between the models, all use inputs related to weather and surface properties. Among surface properties, the initial surface temperature is noted as most influential.

### **1. Simulating Stormwater Runoff Volume and Temperature**

A detailed explanation is provided by Janke et al (2009) for the development of a hydro-thermal model to simulate thermal pollution from a paved surface. The model used a reference stream temperature, rainfall temperature and depth, initial pavement and sub-grade temperatures, pavement and sub-grade thermal diffusivity, and physical characteristics of the pavement (slope,

roughness, length) as inputs to estimate stormwater runoff volume and temperature. Thermal pollution was predicted to within 6% of observed values when applied to a case study using a small parking lot in Minneapolis, Minnesota for an early-evening August rainfall event. Results aligned well with those from the models of other studies, as well as findings from a sensitivity study of the input parameters. The sensitivity study revealed that the results were most sensitive to the temperature inputs and rainfall amount. Janke et al. (2009) found that the low reference temperature of a cold-water stream, high rainfall (atmospheric) and initial pavement temperatures, and a large volume of rainfall create a scenario for highest potential thermal impact. The study stressed the importance of both runoff volume and temperature, as large volumes of runoff may have low temperatures, but still deliver high thermal loads.

## **2. Land Cover Temperature**

One of the most controlling inputs for stormwater thermal pollution estimation is land cover temperature (Herb et al. 2008). This study simulated land surface temperatures for various land cover categories for the purposes of thermal pollution estimation by developing three models: 1) temperature simulation of paved land covers, 2) temperature simulation of bare soil and 3) temperature simulation of vegetated land covers. Temperatures were simulated and tested against measured values for asphalt, concrete, bare soil, tall grass, forest, lawn, and corn for the months of April through October in both dry and wet weather conditions over six years of climate data. All models took into account thermal properties of the surface materials such as thermal conductivity, specific heat, and density as well as surface roughness, albedo, and emissivity. Weather conditions such as solar irradiance, air temperature, wind speed, and dewpoint temperature were also used as major inputs. The vegetated surface temperature model introduced a plant canopy model which accounted for effects to heat fluxes due to shading, re-radiation, and wind sheltering. The models estimated temperatures to within 2°C, with improved results after calibration. A comparison of land cover temperatures was given, ranking the land covers according to their average monthly temperature, average monthly wet weather temperature, average daily maximum temperature, average daily minimum temperature, and average daily amplitude (maximum-minimum) temperature. The comparison of land cover temperatures provides a basis for estimating a comparative potential for thermal pollution contribution among different land covers.

## C. SUMMARY

The review of current literature surrounding stormwater thermal pollution in the urban environment revealed an array of knowledge regarding the significance of stormwater thermal pollution and the contributing hydrothermal mechanisms. Several studies have outlined how urbanization contributes to thermal pollution in streams, resulting in greater temperature fluctuations and greater average temperatures in the summer months (Paul and Meyer 2001; Pluhowski 1970). Studies have also investigated what parameters can be used to predict stormwater thermal pollution, resulting in models that use a number of inputs (Haq and James 2002; Janke et al. 2009; Kieser et al. 2004; Roa-Espinosa et al. 2003). Several of these studies also determined some of the most salient predictors of stormwater thermal pollution that contribute directly to estimations of thermal load (stormwater runoff volume and temperature). Most notable among the predictors are land cover temperature and rainfall/atmospheric temperature, both used as major inputs to all of the stormwater thermal pollution models presented.

## III. DEVELOPMENT OF EFFECTIVE PROCEDURES FOR STORMWATER THERMAL POLLUTION POTENTIAL RISK MAPPING

### A. INTRODUCTION

Thermal pollution of water bodies in urban catchments is a growing water quality concern in the United States. The U.S. Environmental Protection Agency (EPA) and state agencies such as the Virginia Department of Environmental Quality (DEQ) maintain regulatory criteria for various water quality parameters including temperature (USEPA 2016; VADEQ 2014; Virginia Administrative Code 1998). According to the Virginia DEQ Final 2014 305(b)/303(d) Water Quality Assessment Integrated Report (VADEQ 2014), there are many bodies of water identified as impaired for aquatic life due to temperatures in excess of these criteria. Twenty-nine percent of all assessed rivers/streams (6,479 miles), 43% of assessed lake acres (48,555 acres), and 86% of assessed estuarine waters (2,114 square miles) are impaired for aquatic life using dissolved oxygen, pH, temperature, chlorophyll a, nutrients, water column and sediment toxics, toxicity tests, benthics, and submerged aquatic vegetation as indicators for the aquatic life use (VADEQ

2014). In the New River Basin, 13% of river impairments are due to temperature, which is higher than impairments due to benthics, PCBs in fish tissue, mercury in fish tissue, and sedimentation. Temperature is second only to bacteria causes, which are represented in 85% of river impairments (VADEQ 2014, Table 4.3-17).

Aquatic life is dependent on ecosystems that maintain a healthy temperature regime. Temperature assumes a controlling, or at least a modifying role, in most aspects of insect development (i.e. macroinvertebrates) (Vannote and Sweeney 1980). Additionally, water temperature is one of the most important environmental stressors affecting fish. Temperature regimes influence migration, egg maturation, spawning, incubation success, growth, inter- and intraspecific competitive ability, and resistance to parasites, diseases, and pollutants (Armour 1991). Salmonid species, like trout, are among the fish most sensitive to water temperature fluctuations (Jones et al. 2007). Brown Trout (*Salmo trutta*), for example, have an optimum temperature range of 7 to 17 °C and become stressed at temperatures above 19 °C, while temperatures above 26 °C are considered lethal (Roa-Espinosa et al. 2003). While most fish species can tolerate seasonal changes in temperature, rapid spikes in temperature are particularly lethal (Jones et al. 2007).

Due to these negative effects on stream ecology, municipalities are seeking effective means to predict the sources of thermal pollution within their jurisdictional boundaries so that they may efficiently allocate resources for mitigation techniques such as installation of best management practices (BMPs) that have been shown to reduce thermal loading of stormwater runoff (Jones et al. 2007; Long and Dymond 2013). To more effectively implement minimization and mitigation strategies, the salient factors for predicting sources of thermal pollution in surface runoff must be determined prior to application of models evaluating areas of high thermal load potential within urban areas.

## B. BACKGROUND

Previous studies have shown that urbanization has a strong thermal impact on streams (Roa-Espinosa et al. 2003; Pluhowski 1970). Urbanization affects many elements of importance to stream heat budgets, such as removal of riparian vegetation that would otherwise provide



shading and evapotranspiration, decreased groundwater contribution, and increased stormwater runoff that has been heated by contact with warm surfaces (e.g. the “heat island” effect associated with urbanization) (Roa-Espinosa et al. 2003; Pluhowski 1970; Paul and Meyer 2001; Kieser 2004; Kim 1992). According to the study performed by Pluhowski (1970), summertime storms resulted in increased temperature pulses of urban streams by up to 10-15 °C when compared with forested streams in Long Island, New York. Pluhowski also asserted that the precise effect that stormwater runoff will have on the temperature of downstream reaches is a function of the relative volume of stormwater runoff to streamflow, the ambient temperature differences between the two, and whether the stormwater runoff enters the stream as a concentrated mass or whether it is distributed along the channel. Urbanization increases stormwater runoff volume and decreases riparian vegetation – which also affects flow regime, increasing the likelihood of concentrated stormwater entering the stream (Pluhowski 1970; Jones et al. 2007). The effects of the temperature differences and relative volume of stormwater runoff seem to play the largest roles (Jones et al. 2007; Wardynski et al. 2013).

Several studies have been successfully performed to estimate stormwater runoff temperature in urban catchments to determine its effect on stream temperature (Herb et al. 2007; Herb et al. 2008; Janke et al. 2008; Janke et al. 2013). The studies all concluded that land surface temperature plays a significant role in the stormwater runoff temperatures entering the stream. Models that estimate land surface temperature are useful in determining stormwater runoff temperature, since the two parameters are directly related. According to Herb et al. (2008) and Janke et al. (2013), land surface temperature varies by land cover type. Therefore, the land cover types present in an urban catchment can be used to determine the extent to which thermal pollution may potentially occur in a receiving stream from a particular point of interest.

### C. RESEARCH PURPOSE

The current literature provides studies that predict stormwater runoff rates and temperatures to quantify thermal load impacts by taking into account radiative, convective, evaporative, and conductive heat fluxes at the surface (Janke et al. 2008; Roa-Espinosa et al. 2003). These models require a significant number of input parameters including, but not limited to, rainfall

temperature and volume, initial surface temperature, and various other surface properties such as thermal diffusivity, heat capacity, area, slope, and roughness (Janke et al. 2008). Each of these models require different inputs for different rainfall events and multiple iterations for varying surfaces. While these models are effective predictors of stormwater runoff thermal load for a specific rainfall event and surface properties, there remains a need for a simpler procedure – independent of specific rainfall events – to estimate potential locations where thermal pollution might occur throughout a watershed. No literature was found that defines methods for quantifying this potential for thermal pollution along surfaces in an urban watershed. This study develops several procedures that estimate thermal pollution potential (TPP) – a numerical score assigned to areas of interest based on the relative potential for contribution of thermal pollution to the nearest receiving inlet or watershed outlet (pour point) based on hydrothermal processes independent of weather conditions. The resultant TPP values are spatially analyzed in a GIS to produce a TPP risk map. This study also determines the impact of using varying types of input data to determine the transferability of these procedures to other municipalities outside of the study area. The ultimate goal of this research is to provide approachable procedures, that employ little data, to create a TPP risk map for identifying areas with high potential for causing thermal pollution.

Once areas within watersheds that are prone to thermally polluting receiving waters are identified, potential locations for stormwater BMPs that can seek to mitigate the effects of thermal pollution can be identified through use of the TPP risk map. Some BMPs have been shown to reduce runoff temperature by passing water through cooler subsurface media (Wardynski et al. 2013; Long and Dymond 2013). Additional types of BMPs have been shown to mitigate thermal pollution by runoff volume reduction (Jones et al. 2007; Wardynski et al. 2013). The TPP risk map could be used as an action plan element for reduction of thermal pollution to a municipality's receiving streams.

## D. METHODS

This study was performed in three consecutive phases. First, risk factor datasets were identified and obtained for the purpose of developing a thermal pollution potential (TPP) dataset. Second, a

process for TPP calculation was developed using the risk factor datasets as inputs. The datasets were then spatially analyzed in a GIS environment using multiple techniques for TPP risk mapping procedures.

## **1. Data Sources**

The Town of Blacksburg was used as the study site, so much of the data was obtained from their geodatabase (Blacksburg GIS 2015). The data included the following six files:

- The raster-based National Land Cover Database (NLCD 2011 Land Cover) (Multi-Resolution Land Use Consortium 2011)
- The raster-based National Elevation Database (NED 2013)
- A polygon layer representing the Town of Blacksburg's Detailed Land Cover Database (DLCD 2013)
- A polygon layer representing infrastructure-corrected urban watersheds
- A point layer representing stormwater infrastructure nodes (e.g. inlets, manholes, etc.)
- A line layer representing 2-ft contours

The NLCD, a 30-meter resolution land cover data layer that identifies one of 16 classes of land cover for every 30-meter cell in the conterminous United States (Homer et al. 2007), was accessed and downloaded from the Multi-Resolution Land Characteristics Consortium (MRLC) website (MRLC 2011). The NED, a 1/3 arc-second (approx. 10-meter) resolution digital elevation model (DEM), was accessed and downloaded from the United States Geological Survey (USGS) website (U.S. Geological Survey 2013). All other layers were accessed and downloaded from the Town of Blacksburg geodatabase (Blacksburg GIS 2015).

The Town of Blacksburg DLCD (2013) was based on 2013 data releases of high spatial resolution aerial imagery from the Virginia Base Mapping Program (VBMP) via the Virginia Geographic Information Network (VGIN) (VBMP 2016). The DLCD (2013) was created in conjunction with the Blacksburg Stormwater Project for purposes of stormwater modeling and other research by delineating boundaries of land cover types within ArcMap (ESRI 2015).

## 2. Thermal Pollution Potential Development

TPP is a form of risk analysis which assigns a numerical score to individual raster grid cells based on the relative potential for contribution of thermal pollution to the nearest pour point. TPP is designed to assess potential for thermal pollution on a spatial scale, so it is independent of inputs that vary on the event scale such as rainfall temperature and amount and sunlight intensity. The actual measure of how much thermal pollution a surface contributes to runoff is the total heat energy transferred into the runoff from the surface. TPP is not a direct measurement of this energy flux, rather it serves to compare various land covers for their potential to conduct available heat energy to runoff relative to other land covers for any weather condition. The method used to quantify TPP is meant to align with the physical and hydrological processes that govern surface heat energy transfer into runoff from the moment at which the runoff accumulates on a surface to the moment at which the runoff flows into a pour point.

### *(a) Determining Risk Factors*

The heat energy budget for a pavement surface ignoring weather-related inputs is shown in Figure 1a and is adapted from Kieser (2004). Shown in the figure are the thermal energy sources and sinks which TPP accounts for in stormwater runoff: energy input from the surface ( $E_g$ ), energy release to the atmosphere ( $E_s$ ), and energy output to the pour point ( $E_{out}$ ). Figure 1a represents a single grid cell, while Figure 1b combines these grid cells into a small theoretical watershed to demonstrate where these thermal energy sources/sinks occur throughout the system. Figure 1b demonstrates the thermal energy budget if the bottom rightmost cell is the pour point, and the thermal pollution impact of the surface in the top leftmost cell is to be analyzed.

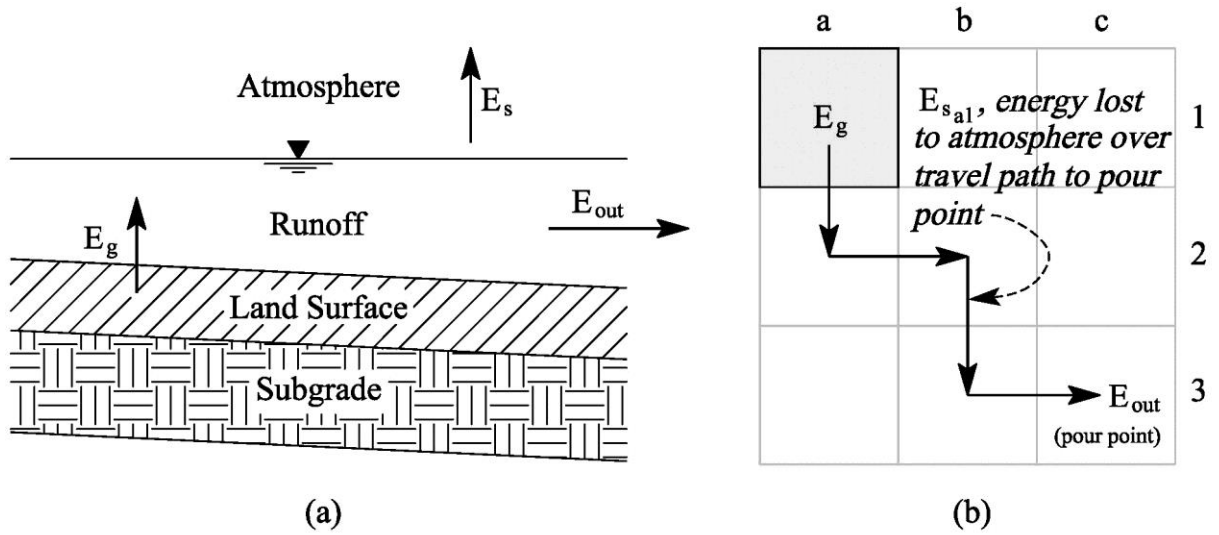


**Figure 3-1. Stormwater runoff thermal energy heat budget ignoring weather-related inputs on a) a single land cover cell (adapted from Kieser 2004) and b) a theoretical watershed of nine land cover grid cells**

Given the comparative nature of TPP analysis, the energy parameters are replaced by models where  $E_g$  is modeled by  $TPP_{LC}$ ,  $E_s$  is modeled by runoff travel time  $t_r$ , and  $E_{out}$  equates to TPP as defined in this paper. TPP therefore relies on  $TPP_{LC}$  and runoff travel time. The  $TPP_{LC}$  parameter is a categorical estimate of potential for transferred heat from a surface. Land cover type dictates the  $TPP_{LC}$ , as heat transfer to runoff above the surface depends on the surface material. Runoff travel time is used to define the time that the heated runoff is exposed to the atmosphere, thereby reducing TPP due to transfer of heat from the runoff to the atmosphere.

Land cover types were categorized by their latent capacity to transfer stored thermal load to runoff to develop  $TPP_{LC}$ . Many variables can play a role in a land cover type's  $TPP_{LC}$ , such as albedo, emissivity, specific heat capacity, and thermal conductivity; however, the most influential variable is a surface's average dry-weather temperature. The potential for heat conduction is controlled by the difference in temperature between surfaces (here, land cover and runoff). The general equation form of heat conduction, also known as Fourier's law, is shown in Equation 1.

$$q = cA(T_1 - T_2)/d \quad (1)$$

where  $q$  is conducted heat [W],  $c$  is thermal conductivity [W/m°C],  $A$  is conduction area [m<sup>2</sup>],  $T_1$  and  $T_2$  are temperatures of the two surfaces [°C], and  $d$  is thickness of receiving material [m].

The categorization of  $TPP_{LC}$  was performed based on a ranking of surfaces with respect to their relative temperatures. The categorization procedure used is supported in literature (Herb et al. 2007; Herb et al. 2008; Janke et al. 2008) where previous studies have suggested ranking various land covers based on contribution to thermal pollution during sample rainfall events. In Herb et al. (2008), average daily maximum surface temperatures were simulated for seven land covers using six years of 15-minute climate data in Albertville, MN in the months of April through October. The average monthly temperatures in the warmest month, July, were used in categorizing  $TPP_{LC}$  and are shown in Table 1 which defines categories, on a normalized scale of 1-10, that represent the  $TPP_{LC}$  assigned to each land cover type in the DLCDC (2013) and the NLCD (2011). Each category groups land cover types from the NLCD (2011) that are similar in type and in  $TPP_{LC}$  to those in the DLCDC (2013) to avoid categorization discrepancies when comparing results from the two datasets.  $TPP_{LC}$  categories six and seven remain empty to enable flexibility if additional categories are necessary that may fall between the developed surfaces and the undeveloped surfaces, or if the categorization procedure needs adjustment depending on the municipality's available land cover data.

**Table 3-1. TPP<sub>LC</sub> categories for DLCD (2013) and NLCD (2011) land cover types assigned using temperature data from Herb et al. (2008)**

<b>TPP<sub>LC</sub></b>	<b>Land Cover (DLCD)</b>	<b>Land Cover (NLCD)</b>	<b>Herb et al. (2008) Land Cover &amp; Temperature (°C)</b>
1	Dense Forest	Woody Wetlands, Emergent Herbaceous Wetlands	Forest (22.3)
2	Light Forest/Tree Canopy	Deciduous Forest, Evergreen Forest, Mixed Forest	Forest (22.3)
3	Brush/Bush, Light Bush/Mulch	Shrub/Scrub, Pasture/Hay, Cultivated Crops	Corn (22.5) / Tall Grass (23.1)
4	Open Space-Lawn	Developed Open Space, Grassland/Herbaceous	Lawn (22.9) / Tall Grass (23.1)
5	Dirt, Gravel	Barren Land-Rock/Sand/Clay, Open Water	Bare Soil (28.6)
6	N/A	N/A	N/A
7	N/A	N/A	N/A
8	Buildings	Developed, Low Intensity	Concrete (31.9)
9	Sidewalk, Other Asphalt/Concrete	Developed, Medium Intensity	Concrete (31.9) / Asphalt (32.9)
10	Road/Parking	Developed, High Intensity	Asphalt (32.9)

Runoff travel time was used to estimate the time within which the runoff is exposed to the atmosphere before reaching the point of analysis (pour point). The velocity method, developed by the Natural Resource Conservation Service (NRCS), formerly the Soil Conservation Service (SCS 1986), was used to determine travel time,  $t_i$ , from each cell to its most downstream cell (the pour point). The velocity method, generally accepted as the standard reference for computation of travel time (Hodges et al. 2015), breaks runoff into three flow regimes: sheet (or “overland”) flow, shallow concentrated flow, and channelized flow. Since channelized flow typically begins at the point of entry to the stormwater conveyance system, only the first two flow regimes, sheet and shallow concentrated, are used for travel time calculations in this study. SCS (1986) suggests that the typical maximum length that runoff can be maintained as sheet flow prior to concentrating is 91.4m (300ft), while Woodward et al. (2010) alternatively suggest a maximum limit of 30.5m (100ft). The alternative maximum limit of 30.5m was used for this study as it was

deemed more appropriate considering the urbanized nature of the study area, where sheet flow is quickly concentrated by curbs and gutters. The shallow concentrated flow velocity is shown by SCS (1986), based on empirical studies, to be proportional to the square root of land slope and a constant, channel  $k$ , that varies based on the predominant land cover (paved or unpaved).

*(b) TPP Calculation*

The calculation procedure for TPP was developed with the goal of reducing the number of input variables while adhering to the thermodynamic processes that govern thermal enrichment of runoff from surfaces. Of particular concern is the total thermal energy received by streams from runoff, since the ultimate goal of mitigation techniques is to reduce this value. TPP, though dimensionless, represents the potential total thermal energy that is received by a point of interest (here, stormwater inlets and watershed outlets) from the runoff originating at a particular surface area (grid cell).  $TPP_{LC}$ , also dimensionless, represents the potential maximum thermal energy that can be received by a volume of runoff from a particular surface area.

TPP is assigned to each grid cell within a subject area; however, the point of analysis is at the point of entry to the stream or stormwater conveyance network (pour point). Therefore, the TPP of each cell depends on that particular cell's impact on a theoretical control volume of runoff that will eventually reach the pour point. Before that theoretical control volume of runoff reaches the pour point, it will travel along the flow path determined by a flow direction grid.  $TPP_{LC}$  is the raw initial value for TPP computations that is based on the land cover potential for heat conduction to runoff, prior to thermal decay, and is defined as the theoretical maximum TPP. Specifically, this is the case when all potential heat in the surface has been conducted to the control volume of runoff and the runoff has not been cooled by contact with the atmosphere. With  $TPP_{LC}$  defined as each grid cell's potential for thermal conduction, and travel time ( $t_i$ ) defined as the time within which the runoff from a particular cell is exposed to the atmosphere, an equation is developed relating the two parameters according to Newton's Law of Cooling. The final equation is designed to account for heat dissipation to the atmosphere as a volume of heated runoff travels along the surface before reaching the pour point. Newton's Law of Cooling relates the rate of change in the temperature of an object to the difference in temperature between the object and its surroundings (Tracy 1972), as shown in Equation 2.



$$\frac{dT}{dt} = -K(T - T_a) \quad (2)$$

where  $T$  = temperature of the object as a function of time [ $^{\circ}\text{C}$ ];  $t$  = time [min];  $K$  = a proportionality constant specific to the object of interest (generally, 0.035 for water near room temperature);  $T_a$  = ambient temperature.

Equation 2 is a simplification of Fourier's Law shown in Equation 1 to represent a rate of heat transfer to the atmosphere from an object that is warmer than ambient air (here, runoff that has been heated by a surface). When the differential equation is solved for the temperature of the object as a function of time, Equation 3 is obtained (Tracy 1972).

$$T(t) = T_a + (T_0 - T_a) \times e^{-Kt} \quad (3)$$

where  $T_0$  = initial temperature of the object (before cooling). The  $T_0$  value represents the temperature of the runoff upon leaving the cell, after the runoff has absorbed all potential heat from the surface within the cell.

There are several assumptions applicable to this process of TPP calculation.

1. First, it is assumed that no cell, besides the cells that contain the pour point, will cause a control volume of runoff to reach its theoretical maximum TPP,  $\text{TPP}_{\text{LC}}$ . Underlying this assumption is that a control volume of runoff that is generated on one of these cells will lose heat to the atmosphere as it travels to the pour point.
2. Additionally, it is assumed that the downstream cells have already cooled to atmospheric conditions by the time the control volume of runoff from upstream reaches the cells. This assumption introduces possible error into the analysis as some surfaces may have enough heat capacity to continue to transfer thermal energy to the upstream control volume of runoff. If this assumption were not used, however, the analysis would require a significant number of other detailed inputs including but not limited to runoff volume, surface conductivity and volume (e.g. pavement depth), and temperature of both the surface and the runoff, as is described in Haq and James (2002). This study proposes a simplified procedure for use by municipalities as a comparative analysis of areas within their jurisdiction, hence the need for this assumption.

3. Another assumption is made when determining the origin of a sample control volume of runoff. It is assumed that the control volume of analyzed runoff originates at each individual cell, based on the typical hydrologic assumption of a homogeneous storm occurring over the entire watershed and generating uniform rainfall, meaning each cell analyzed would receive rainfall and theoretically produce runoff. This assumption ignores intracellular storage related to initial abstractions that may prevent a cell from generating any runoff (e.g. all rainfall is infiltrated). It is worth noting that the land cover categories selected for higher  $TPP_{LC}$  values, though based solely upon surface temperature, also tend to have less available subsurface storage and therefore produce higher volumes of runoff than the land cover categories selected for lower  $TPP_{LC}$  values. For this reason, the assumption may not significantly impact the analysis, as both temperature and runoff volume determine the total thermal pollution contribution (or thermal energy load), and land cover categories of higher  $TPP_{LC}$  tend to exhibit higher values of both.

Since  $TPP_{LC}$  is the potential for thermal conduction to the runoff, it is directly proportional to  $T_0$  from Equation 3, the initial temperature of the object (here, runoff after it has been heated). This is true following the assumption that all potential heat from the surface is transferred to the runoff. Therefore,  $TPP$  and  $TPP_{LC}$  can be substituted for  $T$  and  $T_0$ , respectively. Also, as  $TPP$  is a comparative analysis among land cover cells, and the ambient temperature across adjacent cells is assumed constant, the term  $T_a$  can be replaced by zero, thereby removing the term from the calculation. Again,  $TPP$  is designed to be independent of variable weather conditions. The resulting equation is not a mass-balance; instead, it represents individual cell potential for contribution to thermal pollution. The travel time,  $t_i$ , is solely used to represent time exposed to the atmosphere. Travel time therefore causes decay of  $TPP$ . The final  $TPP$  equation is given in Equation 4.

$$TPP(t) = TPP_{LC} \times e^{-Kt} \quad (4)$$

The cooling proportionality constant,  $K$ , is unitless and represents the rate at which an object dissipates heat to its surroundings. The value is obtained empirically and ranges near 0.03-0.04 for small volumes of heated water. A value of 0.035 is initially assumed for the cooling constant,  $K$ .

### 3. Thermal Pollution Potential Risk Map Development

With the major inputs to TPP defined, multiple analyses were performed to develop TPP risk maps. Methods were performed using a single large catchment, containing smaller subwatersheds, within the Town of Blacksburg known as Central Stroubles Creek Basin. The Central Stroubles Creek Basin was chosen as it represents a significant diversity of land cover types: twelve DLCD (2013) land cover type codes (1-11) out of a total of twelve, and eleven NLCD (2011) land cover type codes (11, 21, 22, 23, 24, 41, 42, 43, 71, 81, and 82) out of a total of sixteen. The analyses varied in how the individual subwatersheds and pour points were defined. Variability in definition of subwatersheds and pour points affected the travel time calculations between method scenarios, while the  $TPP_{LC}$  remained the same throughout. The purpose of the multiple method scenarios was to explore different levels of aggregation of defined inlets and watershed scales to illustrate the effects they had on the computation of TPP for TPP risk mapping.

#### *(a) Input Processing*

A number of input variables are required for travel time calculation using the NRCS velocity method, including flow path length, Manning's roughness coefficient  $n$ , surface slope, 2-year 24-hour rainfall depths, and channel coefficient  $k$  (SCS 1986). The flow length and surface slope variables differed for each method. The Manning's roughness coefficient  $n$ , 2-year 24-hour rainfall, and channel coefficient  $k$  were the same for each method. The 2-year 24-hour rainfall value was assumed to be uniform throughout the watershed and determined to be 6.99cm from NOAA Atlas 14 (National Weather Service). The Manning's roughness coefficient  $n$  was assigned to each DLCD (2013) land cover type based on values determined by previous studies (Chow 1959; FHWA 2013; Moore 2011). The channel coefficient  $k$  was assigned to each DLCD (2013) land cover type according to SCS (1986) for "paved" and "unpaved" land covers. Table 2 lists each DLCD (2013) land cover type with its assigned Manning's  $n$  and channel coefficient  $k$  values along with the source from which the Manning's  $n$  values were derived.

**Table 3-2. Manning’s n and channel k values assigned to DLCD (2013) land cover types**

<b>DLCD Class</b>	<b>Land Cover Description</b>	<b>Manning’s n</b>	<b>Channel k (m/s)</b>	<b>Manning’s n Source</b>
1	Sidewalk	0.013	6.196	Chow (1959)
2	Road/Parking	0.011	6.196	FHWA (2013)
3	Buildings	0.011	6.196	FHWA (2013)
4	Gravel	0.033	6.196	Chow (1959)
5	Other Asphalt/Concrete	0.012	6.196	FHWA (2013)
6	Open Space-Lawn	0.013	4.918	Moore (2011)
7	Dirt	0.030	4.918	Chow (1959)
8	Light Forest/Tree Canopy	0.400	4.918	FHWA (2013)
9	Dense Forest	0.800	4.918	FHWA (2013)
10	Brush/Bush	0.100	4.918	Chow (1959)
11	Light Bush/Mulch	0.060	4.918	Chow (1959)

Each method then used standard procedures for defining flow networks, given by Maidment (2002), including using ESRI ArcMap Spatial Analyst (ESRI 2015) tools to fill sinks, and generate flow direction and flow accumulation grids. A series of python scripts (Python Software Foundation) were written to analyze travel times at the subwatershed-scale for each of the three methods. A slope grid was generated using the Spatial Analyst “Slope” tool. The Spatial Analyst “Flow Length” tool was used to generate flow lengths for each cell. Then the lengths were manipulated to determine sheet flow length and shallow concentrated flow length using recommendations by Woodward et al. (2010). The lengths were used along with land slope, 2-year 24-hour rainfall, Manning’s n, and channel coefficient k to determine inverse velocities for each cell’s sheet flow and shallow concentrated flow, which were then summed together for each cell. Finally, the travel times  $t_t$  were determined by employing the “Flow Length” tool once again, this time using the summed inverse velocity as a weight grid, essentially multiplying the inverse velocity by flow length along the runoff flow path.

*(b) Method 1: Coarse Analysis using Aggregated Inlets for Automatic Drainage Network Extraction*

Method 1 defines subwatersheds using pour points from select receiving inlets, filtered by their proximity to a surface DEM-based drainage network analysis. The drainage network analysis was performed as originally posed by O’Callaghan and Mark (1984) and adopted by Maidment

(2002) for automated subwatershed delineation in ArcMap. This method integrates the 10-m DEM from the NED (2013) and the point layer representing stormwater infrastructure nodes (Blacksburg GIS 2015). The threshold contributing area for flow networks was chosen as nine hectares to represent the start of concentrated flow (O’Callaghan and Mark 1984). The stormwater infrastructure nodes were then used to identify inlets to be used as pour points for subwatershed generation. Only the inlets within 10 meters (one grid cell in the direction of flow) of the flow network were considered for use as pour points; those within 10 meters but not within a flow network cell were moved to the adjacent flow network cell using TauDEM tools (Tarboton 2004). The inlets not within 10 meters of the flow network were excluded from the analysis. Once the pour points were identified, subwatersheds were generated using the Spatial Analyst tool “Watershed”. Travel times were computed using the flow length grids defined by each subwatershed.

Method 1 used a nationally-available surface DEM and a locally-developed infrastructure node layer to determine subwatershed areas. For a municipality, this method may be the least labor-intensive, as all subwatershed delineations can be automated in ArcMap (ESRI 2015) with Python code (Python Software Foundation). This method is reasonably accurate for rural applications; however, in an urban environment, many conveyances do not align with the DEM. Inlets are not always placed at the lowest hydrologic point or at the point of highest flow accumulation according to the DEM analysis. The characteristics of urban hydrology are far more complicated, which can result in significant discrepancies between the hydrologic processes that exist and the hydrologic processes Method 1 assumes. Method 2 was then developed to correct these discrepancies by its use of infrastructure-corrected subwatersheds.

*(c) Method 2: Fine Analysis using Infrastructure-corrected Subwatersheds*

Method 2 defines subwatersheds using infrastructure-corrected subwatershed polygons and performs the analysis without any use of pour points. The infrastructure-corrected subwatershed polygons were created manually using knowledge of the urban landscape and the stormwater conveyance network; see Dymond et al. (2015) for additional information regarding infrastructure-corrected subwatershed delineation in the urban environment. This method also used a 1-m DEM created from 2-ft contours for creation of flow direction grids, slope grids, and

flow length grids in each subwatershed, using ArcMap 10.3.1 (ESRI 2015), for calculation of travel times within each subwatershed.

Implementation of the methodology in Method 2 remains relatively simple since the only other major inputs are the DEM and land cover data. Method 2 uses watershed boundaries likely to be more accurate than those of Method 1 since the boundaries have been adjusted to account for the presence of known infrastructure; however, the computations using input variables from the DEM and land cover dataset are still used to determine the travel times for each cell. Because the DEM does not necessarily match the infrastructure-corrected watershed boundary, there can be discrepancies between logical cell travel times and the location of the cell within the watershed. This is due to a lack of a well-defined pour point or outlet for each watershed. Inner cells tend to flow to multiple cells along the edge of the watershed boundary instead of flowing to a single pour point for the analysis. Method 3 was then developed by using pour points within the infrastructure-corrected subwatersheds.

*(d) Method 3: Fine Analysis using Pour Points for Automatic Drainage Network Extraction within Infrastructure-corrected Subwatersheds*

Method 3 defines subwatersheds using the drainage network analysis similar to Method 1 performed within the infrastructure-corrected subwatersheds used in Method 2. A 1-m DEM was created from 2-ft contours within each infrastructure-corrected subwatershed for drainage network analysis. Select receiving infrastructure inlets and edge-correction pour points were both used for the automated subwatershed delineation using Spatial Analyst tool “Watershed” within each infrastructure-corrected subwatershed. The threshold contributing area was defined as 0.2 hectares, or approximately ½-acre to better represent the smaller catchment size of an urban environment (Pourali et al 2014). The edge-correction pour points are manual additions to the pour points layer created at the most downstream point of the flow networks, with greatest flow accumulation, within each infrastructure-corrected subwatershed with the purpose of providing sufficient subwatershed coverage despite disagreement between the DEM-based drainage network analysis and the infrastructure-corrected subwatersheds. Travel times were computed using the flow length grids defined by each subwatershed generated using the drainage network analysis.

Similar to Method 1, the stormwater infrastructure nodes were used to identify inlets to be used as pour points. Only the inlets within 10 meters (ten grid cells in the direction of flow) of the flow network were considered for use as pour points; those within 10 meters but not within a flow network cell were moved down the flow direction grid using TauDEM tools (Tarboton 2004). The inlets not within 10 meters of the flow network were excluded from the analysis. Since the moved inlets did not provide sufficient coverage for grid cells to be assigned a downstream node (pour point) within each infrastructure-corrected subwatershed, edge-correction pour points were created within each infrastructure-corrected subwatershed. Consequently, most surface grid cells that did not drain to an existing inlet within 10 meters of the flow network drained to the perceived outlet of the infrastructure-corrected subwatershed, as defined by the edge-correction pour points. This procedure did not correct all errors; many gaps still exist because the automatically-generated subwatersheds could not be forced to fill all of the infrastructure-corrected subwatershed areas. These gaps were completely excluded from the analysis because travel time data could not be calculated where subwatersheds were not generated.

Method 3 sought to combine the relative strengths of both Method 1 and Method 2. By using infrastructure-corrected subwatersheds, the subwatershed boundaries were likely to be more accurate than those of Method 1. Also, use of inlet locations as subwatershed pour points provides the surface continuity necessary to direct inter-cell flow to logical outfall locations, every cell is assigned a pour point; however, there exist significant gaps in the data where subwatersheds were not filled out despite the addition of edge-correction pour points. Due to discrepancies between the DEM and infrastructure conditions, no amount of edge-correction pour points could reasonably fill all gaps in the data. Method 3 uses the most inputs, consumes the most data, and requires additional user interaction by placing the edge-correction pour points, making it the most labor-intensive and data-intensive method.

## E. RESULTS AND DISCUSSION

Analysis of the results stemming from this geospatial analysis of TPP resulted in several insights for development of TPP risk maps. The watershed boundaries delineated using each method are

illustrated in Figure 2. Method 1 is the coarsest analysis at 10-m resolution with the fewest subwatersheds. This method takes into account relatively few of the total inlets present, which, along with discrepancies between infrastructure and the DEM, causes a noticeable range in subwatershed size. Method 2 and Method 3 were both performed at 1-m resolution and use the infrastructure-corrected subwatersheds. Method 2 relies solely on the infrastructure-corrected subwatersheds, while Method 3 includes select infrastructure inlets to produce automatically-generated subwatersheds within the infrastructure-corrected subwatersheds. Without exposure to the discrepancies between infrastructure and the DEM, Method 2 is more uniform than Method 1 and more continuous than Method 3 which has noticeable gaps in data (indicated by the empty spaces). Despite the gaps in data, Method 3 has the greatest number of subwatersheds that align both with infrastructure-corrected subwatersheds and the automatically-extracted drainage network based on the DEM. A visual analysis of actual infrastructure locations throughout the Central Stroubles watershed suggested the hydrologic patterns of the watershed differed significantly from what Method 1 indicated, as expected in an urbanized environment, where automated drainage network extraction is error prone. The improvements to subwatershed accuracy from use of infrastructure-corrected subwatersheds were therefore significant. In addition, the flexibility in spatial resolution afforded by Methods 2 and 3 allowed for sensitivity analysis; Methods 2 and 3 were later performed at 10-m resolution for comparison. Method 1 was abandoned for the reasons described above, and Methods 2 and 3 only were used for TPP risk map creation and further analyses.



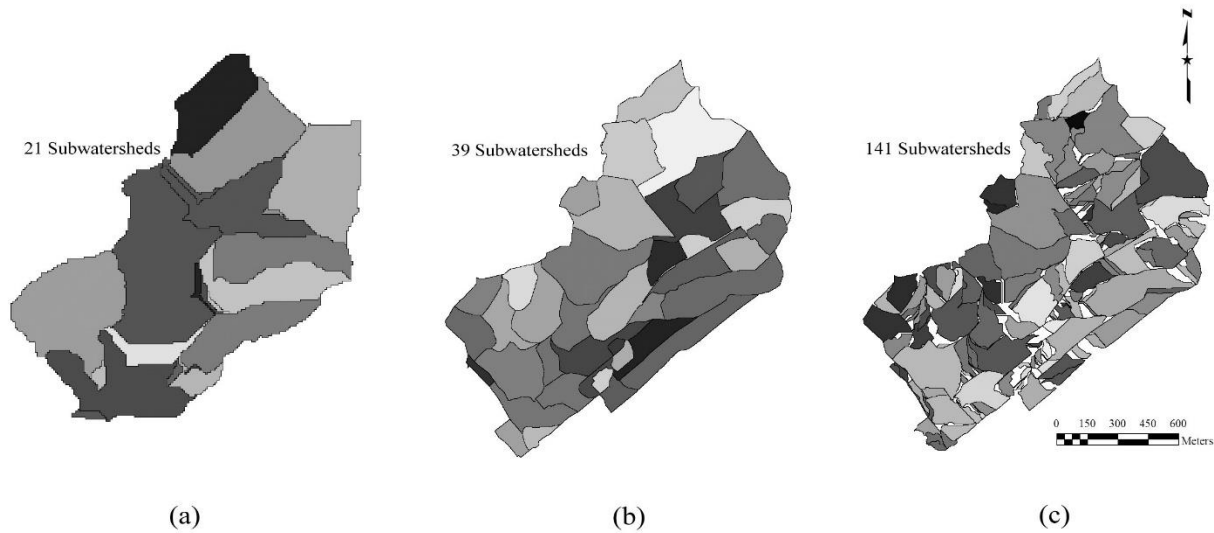


**Figure 3-2. Watershed boundaries developed from a) Method 1, b) Method 2, and c) Method 3.**

The  $TPP_{LC}$  risk map input is shown in Figure 2a and indicates the condition where all cells are at their maximum TPP, when there is no attenuation from exposure to the atmosphere. The final TPP risk maps produced using inputs from Method 2 and Method 3 can be viewed in Figure 2b and Figure 2c, respectively. Note that some areas of high risk on the  $TPP_{LC}$  risk map, indicated by shades of red in the 8-9 and 9-10 bins, have been significantly attenuated in both TPP risk maps while other areas have not. The areas of high risk in the TPP risk maps are characterized by both high  $TPP_{LC}$  and low  $t_t$ . Also note the differences between Figure 2b and Figure 2c. Most apparent is the missing data in Figure 2c as a result of the gaps in watershed delineation in Method 3. These gaps amount to nearly  $0.14 \text{ km}^2$ , meaning about 9% of the total watershed area is excluded from the TPP risk map in Method 3. This Method also appears to exhibit fewer high risk areas, again indicated by shades of red in the 8-9 and 9-10 bins. This result was unexpected, as the smaller subwatersheds from Method 3 resulted in generally lower  $t_t$  values as compared to Method 2, which reduced attenuation of  $TPP_{LC}$ . The full distributions of TPP values across the Central Stroubles watershed for Method 2 and Method 3 at 1-m and 10-m spatial resolutions are shown in Figure 3 where it is noted that Method 3 does exhibit fewer high risk areas, and aggregating resolution to 10-m increases high risk areas in both methods. The fewer high risk areas in Method 3 are due to the excluded data in the gaps as the majority of the areas within

these gaps have high  $TPP_{LC}$ . The increase in high risk area from resolution aggregation is due to a reduction of sinuosity along flow paths, thus reducing the  $t_t$  in the 10-m analysis as compared to the 1-m analysis in both methods.

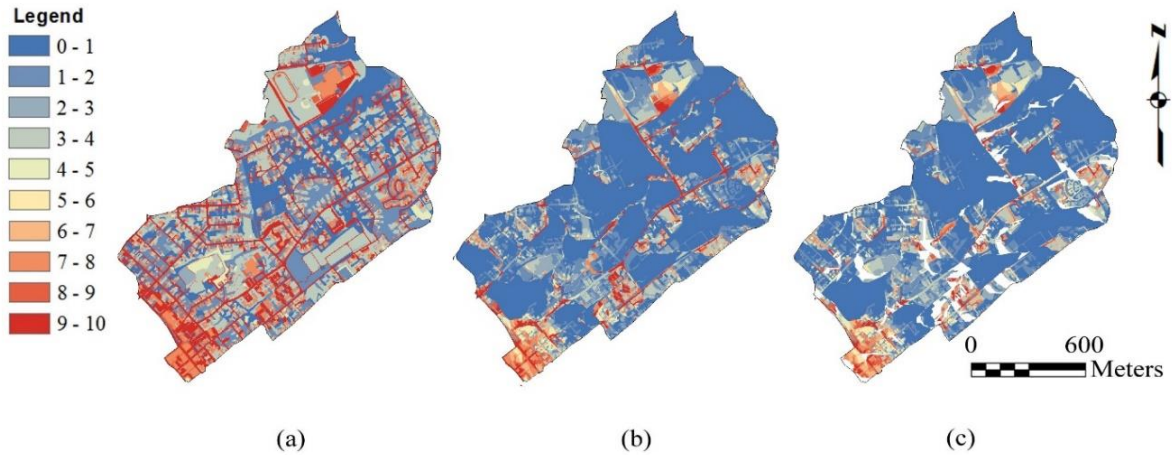


**Figure 3-3. Risk maps of a)  $TPP_{LC}$  derived from DLCD (2013), b) TPP from Method 2, and c) TPP from Method 3. All are at 1-m spatial resolution.**

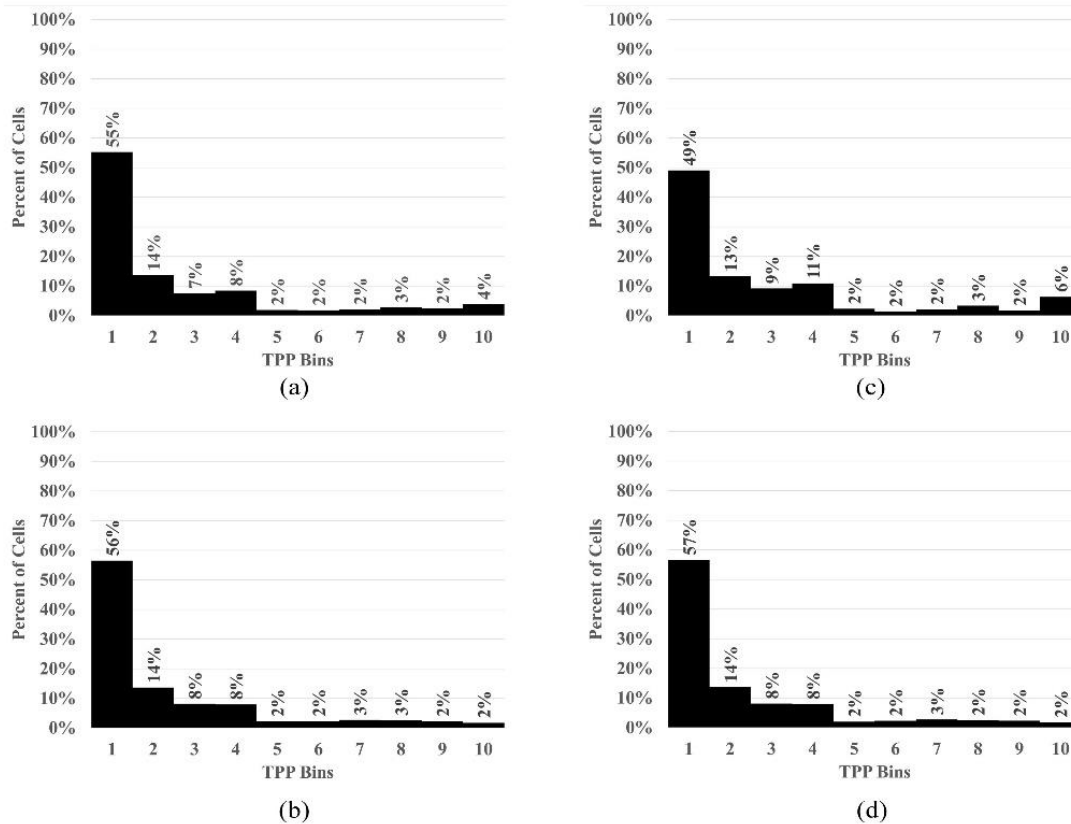


**Figure 3-4. Comparison of TPP frequency distribution across the entire Central Stroubles watershed for a) Method 2 at 10-m resolution, b) Method 2 at 1-m resolution, c) Method 3 at 10-m resolution, and d) Method 3 at 1-m resolution.**

The TPP frequency distribution histograms for both Method 2 and 3 at 1-m and 10-m spatial resolution are shown in Figure 4. Varying spatial resolution of the analysis appeared to more significantly impact the distribution of TPP results than the method of analysis. The total high risk (TPP 8-10) areas represent 4.4% and 7.0% of the watershed in the 1-m and 10-m Method 2 analyses, respectively; whereas, the total high risk areas represent 1.9% and 3.9% of the watershed in the 1-m and 10-m Method 3 analyses, respectively. The rest of the distributions remain fairly similar between methods, which indicates that the additional analysis required for Method 3 is likely not warranted for any significant improvement of accuracy. Method 3 also loses significant data for identification of high risk areas, further supporting Method 2 as the most efficient for identifying high risk areas. Therefore, only Method 2 was used for further sensitivity analyses.

It is important to note how subwatershed scale and land cover distribution within the subwatershed affect TPP values. Histograms were created for two very different subwatersheds that were delineated in Method 2. The histograms are shown in Figure 5, each representing opposing conditions. Subwatershed 1 (Figure 5a) is very small and dominated by high-intensity land covers such as asphalt and buildings, while subwatershed 2 (Figure 5b) is significantly larger and dominated by forest cover. As would be expected, subwatershed 1 is dominated by high TPP values with few in the lower range; and subwatershed 2 is dominated by low TPP values with few in the higher range.

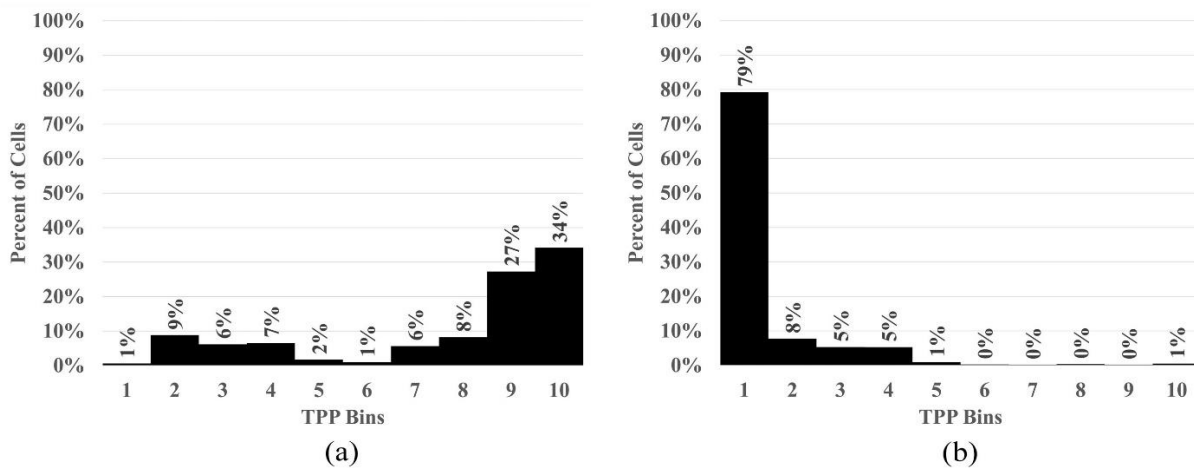


**Figure 3-5. Comparison of TPP frequency distribution using Method 2 at 1-m spatial resolution, for a) Subwatershed 1 and b) Subwatershed 2.**

### 1. K-Value Sensitivity Analysis

The cooling constant,  $K$ , is assumed to be 0.035. This value is not field-verified and could vary according to specific land cover and weather conditions. Therefore, a sensitivity analysis was performed where  $K$  was varied from 0.03 to 0.04. The resulting distributions are shown in Figure 6. While some variation in TPP values is noted, the trends in the data remained relatively unaffected. As was expected, use of a lower  $K$  value (Figure 6a) resulted in higher TPP values than use of a higher  $K$  value (Figure 6b) due to a lessened effect from atmospheric attenuation.

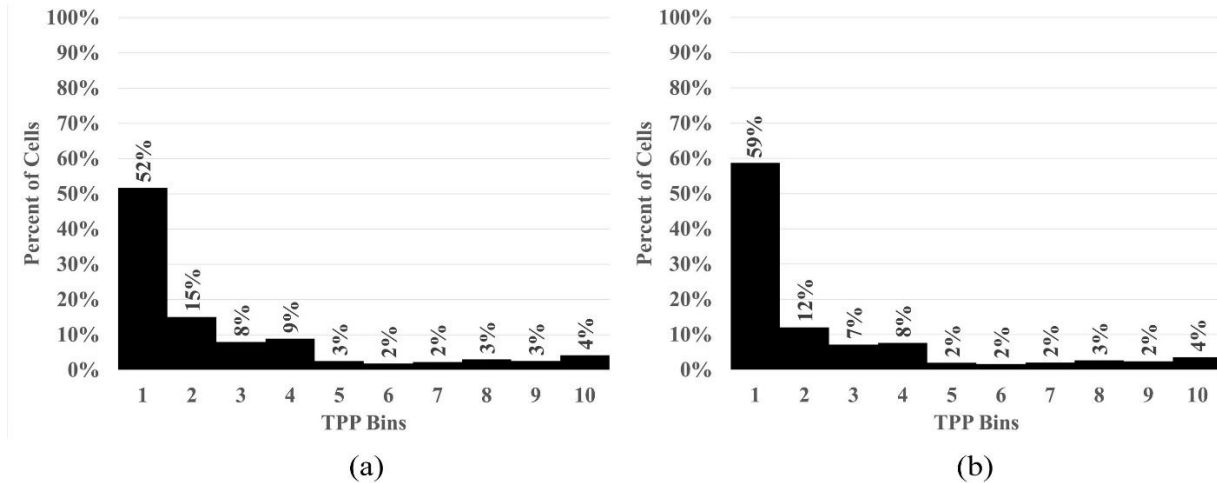


**Figure 3-6. Comparison of TPP frequency distribution from Method 2 at 1-m spatial resolution using separate cooling constant K values, where a) K=0.03 and b) K=0.04.**

## F. CONCLUSIONS

This study has demonstrated a process to quantify thermal pollution potential (TPP) within an urban watershed. It was concluded that both land cover and runoff travel time can be used as factors to estimate an area's potential for thermal pollution contribution to a downstream point of analysis. From this, a thermal pollution potential, TPP, was defined and calculated using a scientific thermal conduction model and spatial analysis in a GIS environment. TPP risk maps were created using various methods, and these methods were analyzed for their effectiveness. Results indicated that Method 2 and Method 3 are both viable options, but that Method 2 proved to be the most advantageous for use by municipalities to determine high TPP risk areas within their watersheds. Method 1 was deemed inadequate for use in urban environments due to the reasons previously discussed. Additionally, results indicated that analysis at 10-m spatial resolution may be sufficient for TPP risk mapping, but it overestimates TPP as compared to 1-m spatial resolution. In regards to land cover inputs, the NLCD (2011) was used solely for determining inputs to be used in travel time calculations. TPP calculations were performed using the NLCD (2011) classes and  $TPP_{LC}$  values presented in Table 1, but the 30-m spatial resolution of the resulting TPP risk maps were deemed too coarse for inclusion in the results. It is unlikely that the NLCD (2011) will provide data detailed enough to produce a TPP risk map to make

informed decisions about where high TPP risk exists within a municipality's watersheds, at least at the scale presented within this study.

The utility of a TPP risk map can be applied by a municipality in the prioritization of thermal pollution mitigation efforts. A TPP risk map gives the municipality the ability to prioritize areas where thermal pollution-mitigating BMPs should be installed, or where other mitigation techniques should be considered. The TPP risk map is used as an action plan element for eventual reduction of thermal pollution to receiving streams. While attempts to trace thermal pollution throughout a watershed using field methods would be very costly and perhaps even futile to a municipality without an idea where to focus their observations, a TPP risk map determines areas of high risk using theoretical hydrologic and thermal processes without the need for field observations. As was expected in this study, areas of high TPP correlated with areas of high-intensity land cover and low travel times before reaching the pour point. A TPP risk map could be used to focus field observations for calibration and eventual determination of the major sources of thermal pollution. The municipality could then focus its resources on the areas of greatest impact. The TPP risk mapping process can be used by any municipality with access to the necessary input data and expertise.

## IV. CONCLUSION

### A. IMPLICATIONS

This study has demonstrated a process to quantify thermal pollution potential (TPP) within an urban watershed. It was concluded that both land cover and runoff travel time play an important role in estimating an area's potential for thermal pollution contribution to a downstream point of analysis. Using these inputs, a thermal pollution potential, TPP, was defined and calculated using a scientific thermal conduction model and spatial analysis in a GIS environment. TPP risk maps were created using various methods, and these methods were analyzed for their effectiveness. Results indicated that Method 2 and Method 3 are both viable options, but that Method 2 proved to be the most advantageous for use by municipalities to determine high TPP risk areas within their watersheds. Method 1 was deemed inadequate for use in urban environments. Additionally, results indicated that analysis at 10-m spatial resolution may be sufficient for TPP risk mapping,

but it overestimates TPP as compared to 1-m spatial resolution. TPP calculations were performed using the NLCD (2011) classes and  $TPP_{LC}$  values presented in Table 1, but the 30-m spatial resolution of the resulting TPP risk maps were deemed too coarse for inclusion in the results. It is unlikely that the NLCD (2011) will provide data detailed enough to produce a TPP risk map to make informed decisions about where high TPP risk exists within a municipality's watersheds, at least at the scale presented within this study.

The utility of a TPP risk map can be realized by a municipality in the prioritization of thermal pollution mitigation efforts. A TPP risk map gives the municipality the ability to prioritize areas where thermal pollution-mitigating BMPs should be installed, or where other mitigation techniques should be considered. The TPP risk map is used as an action plan element for eventual reduction of thermal pollution to receiving streams. While attempts to trace thermal pollution throughout a watershed using field methods would be very costly and perhaps even futile to a municipality without an idea where to focus their observations, a TPP risk map determines areas of high risk using theoretical hydrologic and thermal processes without the need for field observations. As was expected in this study, areas of high TPP correlated with areas of high-intensity land cover and low travel times before reaching the pour point. A TPP risk map could be used to focus field observations for calibration and eventual determination of the major sources of thermal pollution. The municipality could then focus its resources on the areas of greatest impact. The TPP risk mapping process can be used by any municipality with access to the necessary input data and expertise.

## B. FUTURE WORK

While this study has produced promising results for thermal pollution potential risk mapping, there exist many possible areas for further research on thermal pollution potential and thermal pollution potential risk analysis. Land cover temperatures, and how land covers are used for formulation of relative potential for thermal pollution contribution,  $TPP_{LC}$ , could benefit from further studies.  $TPP_{LC}$  is based on studies that model land cover temperatures in regard to their effects on stormwater runoff thermal loading. Further research on land cover temperatures and their relative potentials for heat transfer to stormwater runoff would be beneficial for calibration of  $TPP_{LC}$ . The relative effects of land cover on stormwater thermal pollution may vary by region,

and some municipalities may have different land cover categories that are not represented in this study. Travel time ( $t_i$ ), was calculated using several methods that are generally accepted by the scientific community, but other methods may exist and warrant further study. Travel time computation remains a challenge in urban watersheds due to the complex nature of urban hydrology, and more research is needed to develop effective procedures for determining travel times throughout urban watersheds.

While TPP analysis presented in this study is strongly founded on theory, field observations may allow adjustment or calibration of the equation, particularly the value of the cooling constant,  $K$ , used. Observations of runoff volume and temperature performed at the pour points of various subwatersheds could validate the equation and provide calibration data to better estimate the cooling constant  $K$ , especially during “worst-case scenario” conditions that exist when air/rainfall temperature and solar radiation are high before and during rainfall.

Finally, on a broader scale, future TPP analysis could incorporate downstream effects to stormwater thermal pollution as a result of various sources and sinks of thermal load throughout the storm sewer network. The analyses performed in this study calculated a TPP for subwatershed areas according to their potential for thermal loading to the subwatershed outlet, which may or may not be part of a natural stream. The subwatershed outlet is often an infrastructure inlet that leads to an underground network of pipes as part of the storm sewer system before reaching a natural stream, as is common in urban environments. There exists the potential for changes in thermal load to occur within the storm sewer system before the runoff reaches the natural stream environment. Sabouri et al (2013) studied the thermal effects of underground sewer systems on runoff and found that there is generally a cooling effect as a result of heat transfer between runoff and the relatively cool underground pipes. While knowledge of the potential for thermal pollution contribution to the subwatershed outlet is useful, and is related to the potential for thermal pollution contribution to the receiving stream, a more robust model that accounts for thermal pollution sources and sinks along the storm sewer system could be more useful for determining potential for thermal pollution contribution to the receiving stream. That said, there are more thermal pollution sources and sinks in the storm sewer system than underground pipes.



Structures such as culverts, lined channels, manholes, BMPs such as detention ponds, underground detention facilities, swales, bioretention, infiltration devices, filters, constructed wetlands, and the like all are potentially significant sources and sinks of thermal pollution. While the thermal effects on stormwater runoff of several of these devices has been studied on an individual basis, very little work has been done to evaluate the potential thermal effects of these devices on the storm sewer system scale to determine their combined downstream effects to the stormwater that enters the receiving stream. Evaluating all these downstream thermal effects was beyond the scope of this project, but a future model that considers each would expand the understanding of the transfer of thermal load throughout the conveyance system.

### C. FINAL WORDS

Perhaps the greatest challenge to future TPP research is considering all the aforementioned areas for improvement while maintaining a risk analysis procedure that is relatively simple to use and does not significantly burden a municipality's resources. While stormwater quality is a growing concern, other areas of infrastructure vie for the resources of a municipality. Future TPP research should continue to be mindful of the limitations posed by competing interests by providing a resource-effective means by which a municipality can identify areas for stormwater thermal pollution mitigation efforts.

## REFERENCES

- Armour, Carl L., 1991. "Guidance for Evaluating and Recommending Temperature Regimes to Protect Fish". *Washington, D.C.: U.S. Dept. of the Interior, Fish and Wildlife Service.*
- Blacksburg GIS Database, 2015. [http://www.gis.lib.vt.edu/gis\\_data/Blacksburg/GISPage.html](http://www.gis.lib.vt.edu/gis_data/Blacksburg/GISPage.html).
- Dymond, R. L., Aguilar, M. F., Bender, P., and Hodges, C., 2015. "Roanoke Urban Stormwater Research: Phase II Final Report".
- Environmental Systems Resource Institute (ESRI), 2015. ArcGIS ArcMap 10.3.1 [Computer software].
- Federal Highway Administration (FHWA), 2013. "Hydraulic Engineering Circular No. 22, 3<sup>rd</sup> Ed. Urban Drainage Design Manual".
- Haq, R. and James, W., 2002. "Thermal Enrichment of Stream Temperature by Urban Storm Waters". *Global Solutions for Urban Drainage*: pp. 1-11.
- Herb, William R., Janke, Ben, Mohseni, Omid, and Stefan, Heinz G., 2007. "Estimation of Runoff Temperatures and Heat Export from Different Land and Water Surfaces." *St. Anthony Falls Laboratory Project Report No. 488.*
- Herb, William R., Janke, Ben, Mohseni, Omid, and Stefan, Heinz G., 2008. "Ground Surface Temperature Simulation for Different Land Covers." *Journal of Hydrology* 356.3: 327-43.
- Hodges, C., McDonald, W., Dymond, R., and Hancock, K. (2015). "Improved Methods of Parameterization for Estimating the Magnitude and Frequency of Peak Discharges in Rural Ungaged Streams." *Journal of Hydrologic Engineering.*
- Homer, Collin, Dewitz, Jon, Fry, Joyce, Coan, Michael, Nazmul Hossain, Larson, Charles, Herold, Nate, McKerrow, Alexa, VanDriel, Nick J., and Wickham, James, 2007. "Completion of the 2001 National Land Cover Database for the Conterminous United States." *Photogrammetric Engineering & Remote Sensing*, April, 337–341.
- Janke, Benjamin D., Herb, William R., Mohseni, Omid, and Stefan, Heinz G., 2008. "Simulation of Heat Export by rainfall–runoff from a Paved Surface." *Journal of Hydrology* 365.3:195-212.

- Janke, Benjamin D., Herb, William R., Mohseni, Omid, & Stefan, Heinz G., 2013. "Case Study of Simulation of Heat Export by Rainfall Runoff from a Small Urban Watershed Using MINUHET". *Journal of Hydrologic Engineering*, 18(8), 995–1006.
- Jones, Matthew P., William F. Hunt, and Jonathan T. Smith, 2007. "The Effect of Urban Stormwater BMPs on Runoff Temperature in Trout Sensitive Waters." *World Environmental and Water Resources Congress 2007*.
- Kieser, MS., 2004. "Stormwater Thermal Enrichment in Urban Watersheds." *Water Intelligence Online*.
- Kim, H. H., 1992. "Urban heat island." *International Journal of Remote Sensing*, 13(12), 2319-2336.
- Long, Daniel L. and Randel L. Dymond, 2013. "Thermal Pollution Mitigation in Cold Water Stream Watersheds Using Bioretention". *Journal of the American Water Resources Association (JAWRA)* 50(4): 977-987.
- Maidment, D. R., 2002. Arc hydro: GIS for water resources. *ESRI Press*, Redlands, CA.
- Multi-Resolution Land Use Consortium (MRLC), 2011. "National Land Cover Database (NLCD)." [http://www.mrlc.gov/nlcd11\\_data.php](http://www.mrlc.gov/nlcd11_data.php).
- O'callaghan, J. F., and Mark, D. M., 1984. "The extraction of drainage networks from digital elevation data." *Computer Vision, Graphics, and Image Processing*, 27(2), 247.
- Paul, Michael J., and Meyer, Judy L., 2001. "Streams in the Urban Landscape." *Urban Ecology*, no. 32: 207–231. doi:10.1007/978-0-387-73412-5\_12.
- Pluhowski, Edward J., 1970. "Urbanization and Its Effect on the Temperature of the Streams on Long Island, New York." *Washington, D.C.: USGS Professional Paper*.
- Pourali, S. H., Arrowsmith, C., Mitchell, D., and Matkan, A. A., 2014. "Modelling An Overland Water Flow Path In An Urban Catchment Using GIS." *An International Journal (GIJ)*, (41), 2014–1.
- Python Software Foundation. Python Language Reference, version 2.7. <http://www.python.org>.
- Roa-Espinosa, A., Norman, J.M., Wilson, T.B., and Johnson, K., 2003. "Predicting the impact of urban development on stream temperature using a thermal urban runoff model (TURM)." *Methods*: 369-389.

- Soil Conservation Service (SCS), 1986. "Urban hydrology for small watersheds." *Technical Release No. 55, U.S. Dept. of Agriculture, Washington, DC.*
- Tarboton, D.G., 2004. TauDEM, terrain analysis using digital elevation models. *ArcGIS Extension. Version 5.*
- Tracy, C. R., 1972. "Newton's Law: Its Application for Expressing Heat Losses from Homeotherms." *BioScience*, 22(11), 656–659.
- USEPA, 2016. "NPDES Stormwater Program." *Environmental Protection Agency.*
- U.S. Geological Survey, 2013. USGS NED n38w081 1/3 arc-second 2013 1 x 1 degree ArcGrid: *U.S. Geological Survey: Reston, VA.*
- VADEQ, 2014. "2014 305(b)/303(d) Water Quality Assessment Integrated Report."
- VBMP, 2016. "Orthoimagery." *Virginia Information Technologies Agency.*
- Vannote, Robin L., and Sweeney, Bernard W., 1980. "Geographic Analysis of Thermal Equilibria: A Conceptual Model for Evaluating the Effect of Natural and Modified Thermal Regimes on Aquatic Insect Communities." *The American Naturalist* 115 (5): 667–695. doi:10.1086/283591.
- Virginia Administrative Code, 1998. "Virginia Administrative Code." 1998. LIS >> Administrative Code >> 9VAC25-260-50.
- Wardynski, Brad J., Ryan J. Winston, and William F. Hunt, 2013. "Internal Water Storage Enhances Exfiltration and Thermal Load Reduction from Permeable Pavement in the North Carolina Mountains." *Journal of Environmental Engineering* 139.2: 187-95.

## APPENDIX A – METHOD 2 PYTHON SCRIPTS

```
                                ExtractByAttributes_Watersheds.py
# Name: ExtractByAttributes_Watersheds.py
# Description: Extracts the cells of a raster based on a query of watershed number.
# Requirements: Spatial Analyst Extension

# Import system modules
import arcpy
from arcpy import env
from arcpy.sa import *

# Set environment settings
env.workspace = "E:\Thesis\GIS\Thesis_Trial6_Method2_1m"
env.overwriteOutput = True

# Check out the ArcGIS Spatial Analyst extension license
arcpy.CheckOutExtension("Spatial")

# Set local variables
inRaster = arcpy.Raster("Subbasins_CS.tif")
cursor = arcpy.SearchCursor("Subbasins_CS.tif")

# Execute
row = cursor.next()
counter=int(0)
SQL = ["OID = 0", "OID = 1", "OID = 2", "OID = 3", "OID = 4", "OID = 5", "OID = 6",
"OID = 7", "OID = 8", "OID = 9", "OID = 10", "OID = 11", "OID = 12", "OID = 13",
"OID = 14", "OID = 15", "OID = 16", "OID = 17", "OID = 18", "OID = 19", "OID = 20",
"OID = 21", "OID = 22", "OID = 23", "OID = 24", "OID = 25", "OID = 26", "OID = 27",
"OID = 28", "OID = 29", "OID = 30", "OID = 31", "OID = 32", "OID = 33", "OID = 34",
"OID = 35", "OID = 36", "OID = 37", "OID = 38"]

while row:
    print(str(row.getValue("OID")))
    attExtract = ExtractByAttributes(inRaster, SQL[counter])
    attExtract.save("E:\Thesis\GIS\Thesis_Trial6_Method2_1m\Watersheds\Watershed_"+str(
row.getValue("OID"))+".tif")
    row = cursor.next()
    counter=counter+1
```

```

                                RasterToPolygon_Watersheds.py
# Name: RasterToPolygon_Watersheds.py
# Description: Converts individual watershed rasters to polygon features.
# Requirements:

# Import system modules
import arcpy
import glob
import os
from arcpy import env
from arcpy.sa import *

# Set environment settings
env.workspace = "E:\Thesis\GIS\Thesis_Trial6_Method2_1m\Watersheds"
env.overwriteOutput = True

# Check out the ArcGIS Spatial Analyst extension license
arcpy.CheckOutExtension("Spatial")

# Set local variables
rasters = arcpy.ListRasters("Watershed_*", "TIF")

# Execute
for watershed in rasters:
    print(watershed)
    arcpy.env.snapRaster = watershed
    outNamefull = os.path.splitext(os.path.basename(watershed))[0]
    outName = outNamefull.replace("Watershed", "")
    arcpy.RasterToPolygon_conversion(watershed,
"E:\Thesis\GIS\Thesis_Trial6_Method2_1m\Watersheds\WatershedPoly"+outName+".shp",
"NO_SIMPLIFY", "VALUE")

```

## Clip\_Fdir\_byWatersheds.py

```
# Name: Clip_Fdir_byWatersheds.py
# Description: Clips the standard flow direction grid by the individual watershed polygon
features.
# Requirements:

# Import system modules
import arcpy
import glob
import os
from arcpy import env

# Set environment settings
env.workspace = "E:\Thesis\GIS\Thesis_Trial6_Method2_1m\Watersheds"
env.overwriteOutput = True
arcpy.env.compression = "NONE"

# Execute
for watershed in
glob.glob("E:\Thesis\GIS\Thesis_Trial6_Method2_1m\Watersheds\watershedpoly_*.shp"):
    print(watershed)
    outNamefull = os.path.splitext(os.path.basename(watershed))[0] outName =
    outNamefull.replace("watershedpoly", "")
    output =
arcpy.Clip_management(in_raster="E:/Thesis/GIS/Thesis_Trial6_Method2_1m/Fdir_CS.tif ",
rectangle="#",
out_raster="E:/Thesis/GIS/Thesis_Trial6_Method2_1m/Watersheds/fdir"+outName+".tif",
in_template_dataset=watershed, nodata_value="#", clipping_geometry="ClippingGeometry",
maintain_clipping_extent="NO_MAINTAIN_EXTENT")
    print(output)
```

## Flength\_Watershed.py

```
# Name: Flength_Watershed.py
# Description: Generates flow length using SA flow length tool for each watershed's flow
direction grid.
# Requirements: Spatial Analyst

# Import system modules
import arcpy
import glob
import os
from arcpy import env
from arcpy.sa import *

# Set environment settings
env.workspace = "E:\Thesis\GIS\Thesis_Trial6_Method2_1m\Watersheds"
env.overwriteOutput = True
arcpy.env.compression = "NONE"

# Check out the ArcGIS Spatial Analyst extension license
arcpy.CheckOutExtension("Spatial")

# Set local variables
rasters = arcpy.ListRasters("fdir*", "TIF")

# Execute
for fdir in rasters:
    print(fdir)
    arcpy.env.snapRaster = fdir
    outNamefull = os.path.splitext(os.path.basename(fdir))[0]
    outName = outNamefull.replace("fdir", "")
    output = FlowLength(fdir, "DOWNSTREAM", "")
    output.save("flength"+outName+".tif")
```



## Sheet\_Length.py

```
# Name: Sheet_Length.py
# Description: Generates sheet lengths per watershed flow length grid according to an
approximate limitation of 100 feet.
# Requirements: Spatial Analyst

# Import system modules
import arcpy
import glob
import os
from arcpy import env
from arcpy.sa import *

# Set environment settings
env.workspace = "E:\Thesis\GIS\Thesis_Trial6_Method2_1m\Watersheds"
env.overwriteOutput = True
arcpy.env.compression = "NONE"

# Check out the ArcGIS Spatial Analyst extension license
arcpy.CheckOutExtension("Spatial")

# Set local variables
rasters = arcpy.ListRasters("flength*", "TIF")

# Execute
for flength in rasters:
    print(flength)
    arcpy.env.snapRaster = flength
    outNamefull = os.path.splitext(os.path.basename(flength))[0]
    outName = outNamefull.replace("flength", "")
    output = Con(Raster(flength) >= 100, float(100), Raster(flength))
    output.save("Sheet_Length"+outName+".tif")
```

## Conc\_Length.py

```
# Name: Conc_Length.py
# Description: Generates concentrated flow regime lengths per watershed flow length grid
according to an approximate limitation of sheet flow of 100 feet.
# Requirements: Spatial Analyst

# Import system modules
import arcpy
import glob
import os
from arcpy import env
from arcpy.sa import *

# Set environment settings
env.workspace = "E:\Thesis\GIS\Thesis_Trial6_Method2_1m\Watersheds"
env.overwriteOutput = True
arcpy.env.compression = "NONE"

# Check out the ArcGIS Spatial Analyst extension license
arcpy.CheckOutExtension("Spatial")

# Set local variables
rasters = arcpy.ListRasters("flength*", "TIF")

# Execute
for flength in rasters:
    print(flength)
    arcpy.env.snapRaster = flength
    outNamefull = os.path.splitext(os.path.basename(flength))[0]
    outName = outNamefull.replace("flength", "")
    output = Con(Raster(flength) > 100, (Raster(flength) - float(100)), 0)
    output.save("Conc_Length"+outName+".tif")
```

## Sheet\_InvVel.py

```
# Name: Sheet_InvVel.py
# Description: Outputs inverse velocity grid for sheet flow regime within each watershed.
# Requirements: Spatial Analyst

# Import system modules
import arcpy
import glob
import os
from arcpy import env
from arcpy.sa import *

# Set environment settings
env.workspace = "E:\Thesis\GIS\Thesis_Trial6_Method2_1m\Watersheds"
env.overwriteOutput = True
arcpy.env.compression = "NONE"

# Check out the ArcGIS Spatial Analyst extension license
arcpy.CheckOutExtension("Spatial")

# Set local variables
mannings = "E:\Thesis\GIS\Thesis_Trial6_Method2_1m\Mannings_n.tif" slope =
"E:\Thesis\GIS\Thesis_Trial6_Method2_1m\Slope_1m.tif"
rasters = arcpy.ListRasters("Sheet_Length*", "TIF")

# Execute
for shtlength in rasters:
    print(shtlength)
    arcpy.env.snapRaster = shtlength
    outNamefull = os.path.splitext(os.path.basename(shtlength))[0]
    outName = outNamefull.replace("Sheet_Length", "")
    output = (0.42 * Power((Raster(mannings) * Raster(shtlength)), 0.8)) / (Power(2.75, 0.5) *
Power(Raster(slope), 0.4)) / Raster(shtlength)
    output.save("Sheet_InvVel"+outName+".tif")
```

## Conc\_InvVel.py

```
# Name: Conc_InvVel.py
# Description: Outputs inverse velocity grid for shallow concentrated flow regime.
# Requirements: Spatial Analyst

# Import system modules
import arcpy
import glob
import os
from arcpy import env
from arcpy.sa import *

# Set environment settings
env.workspace = "E:\Thesis\GIS\Thesis_Trial6_Method2_1m\Watersheds"
env.overwriteOutput = True
arcpy.env.compression = "NONE"

# Check out the ArcGIS Spatial Analyst extension license
arcpy.CheckOutExtension("Spatial")

# Set local variables
channelk = "E:\Thesis\GIS\Thesis_Trial6_Method2_1m\Channel_k.tif"
slope = "E:\Thesis\GIS\Thesis_Trial6_Method2_1m\Slope_1m.tif"

# Execute
output = (1 / (Raster(channelk) * Power(Raster(slope), 0.5))) / 60
output.save("Conc_InvVel.tif")
print("done")
```

## Total\_InvVel.py

```
# Name: Total_InvVel.py
# Description: Outputs total inverse velocity grid for both sheet and shallow concentrated flow
regimes within each watershed.
# Requirements: Spatial Analyst

# Import system modules
import arcpy
import glob
import os
from arcpy import env
from arcpy.sa import *

# Set environment settings
env.workspace = "E:\Thesis\GIS\Thesis_Trial6_Method2_1m\Watersheds"
env.overwriteOutput = True
arcpy.env.compression = "NONE"

# Check out the ArcGIS Spatial Analyst extension license
arcpy.CheckOutExtension("Spatial")

# Set local variables
Conc_InvVel = "E:\Thesis\GIS\Thesis_Trial6_Method2_1m\Watersheds\Conc_InvVel.tif"
Sheet_InvVel = arcpy.ListRasters("Sheet_InvVel*", "TIF")

# Execute
for invVel in Sheet_InvVel:
    print(invVel)
    arcpy.env.snapRaster = invVel
    outNamefull = os.path.splitext(os.path.basename(invVel))[0]
    outName = outNamefull.replace("Sheet_InvVel", "")
    output = Raster(invVel) + Raster(Conc_InvVel)
    output.save("Total_InvVel"+outName+".tif")
```

## TravelTime\_Watershed.py

```
# Name: TravelTime_Watershed.py
# Description: Outputs total travel time (in minutes) from each cell to the pour point per
watershed.
# Requirements: Spatial Analyst

# Import system modules
import arcpy
import glob
import os
from arcpy import env
from arcpy.sa import *

# Set environment settings
env.workspace = "E:\Thesis\GIS\Thesis_Trial6_Method2_1m\Watersheds"
env.overwriteOutput = True
arcpy.env.compression = "NONE"

# Check out the ArcGIS Spatial Analyst extension license
arcpy.CheckOutExtension("Spatial")

# Set local variables
watersheds = arcpy.ListRasters("fdir*", "TIF")
invVel = arcpy.ListRasters("Total_InvVel*", "TIF")

# Execute
count = int(0)

for fdir in watersheds:
    print(invVel[count])
    arcpy.env.snapRaster = fdir
    outNamefull = os.path.splitext(os.path.basename(fdir))[0]
    outName = outNamefull.replace("fdir", "")
    output = FlowLength(fdir, "DOWNSTREAM", invVel[count])
    output.save("Tto_" + outName + ".tif")
    count = count + 1
```